ISSN 1061-933X, Colloid Journal, 2008, Vol. 70, No. 1, pp. 55–63. © Pleiades Publishing, Ltd., 2008.
Original Russian Text © A.N. Novruzov, O.R. Rakhmanova, A.E. Galashev, 2008, published in Kolloidnyi Zhurnal, 2008, Vol. 70, No. 1, pp. 61–70.

Computer Study of the Absorption of Ethane by Aqueous Ultradispersed Medium: IR Spectra

A. N. Novruzov, O. R. Rakhmanova, and A. E. Galashev

Institute of Industrial Ecology, Ural Branch, Russian Academy of Sciences, ul. S. Kovalevskoi 20a, Yekaterinburg, 620219 Russia

Received March 23, 2007

Abstract—Absorption of ethane molecules by water clusters containing 10–20 molecules is studied by the molecular dynamics method. The $(H_2O)_n$ (I), $C_2H_6(H_2O)_n$ (II), and $(C_2H_6)_2(H_2O)_n$ (III) cluster systems are composed on the basis of specific statistical weights. Spectral characteristics of system and single clusters are determined in the frequency range of $0 \le \omega \le 1000$ cm^{-1}. In this frequency range, both real and imaginary parts of dielectric permittivity decrease monotonically after the absorption of C_2H_6 molecules by an aqueous ultradispersed system. Integral coefficient of IR absorption increases, while average (over frequency) reflection coefficient decreases after the absorption of ethane molecules. The intensity of IR scattering by the systems of clusters containing C_2H_6 molecules lowers. Maximal values of radiation power for water clusters with various sizes are balanced with the capture of ethane molecules by the clusters, whereas oscillations in the size dependence of the density of electrons that are active with respect to IR radiation decrease.

DOI: 10.1134/S1061933X08010092

INTRODUCTION

Water vapor is the main greenhouse gas of Earth's troposphere. Up to 95% of the greenhouse effect is created by none other than H_2O. Characteristic frequency of intramolecular vibrations belongs to the main characteristics of the ability of molecules to absorb infrared (IR) radiation from the planet's surface. In the infrared absorption, 1595 and 3756 cm^{-1} high-intensity frequencies are observed for water vapor [1]. The spectrum of thermal Earth's radiation corresponding to 280 K is ended actually in the vicinity of 2500 cm^{-1}. The frequency of translational vibrations of molecules (in the condensed state) is usually limited, i.e., $\omega < 1000$ cm^{-1} [2]. As a rule, higher frequencies correspond to intramolecular vibrations. The absorption of radiation in the near-IR region by water dimers in the atmosphere was registered in [3] and confirmed in [4] under laboratory conditions. Data of laboratory measurements on the absorption of the continuous radiation band by water vapor in the 3000–4200 cm^{-1} range were reported in [5]. These measurements reliably confirm the substantial contribution of water dimers to the continuous radiation band in a given spectral range [6].

According to the theory of homogeneous nucleation [7], water clusters of subcritical sizes should exist in the Earth's atmosphere in dynamic equilibrium. Microscopic droplets are formed from clusters of critical sizes. These droplets remain liquid at a temperature lower than the melting temperature. A decrease in the melting temperature of small particles is explained by the surface effect. The absence of reliable data on cluster distribution in Earth's atmosphere [8] does not allow for unambiguous interpretation of many features of continuous absorption spectrum for water vapor observed in the IR region [6]. Regardless of the fact that many classical models were developed for the simulation of liquid water [9–12], the model, which could reproduce all its anomalous properties in not yet created. The manifestation of differences in the behavior of water at different dimensional scales is its inherent property [13]. For example, when dissolving biomolecules in water, a significant role is played by the nearest environment that consists of water molecules located at short distances and involved in the formation of hydrogen bonds. However, the manifestation of the "hydrophobic" effect needs longer organization of the system at larger scales. For example, the hydrophobic effect is exhibited when dissolving ethane in water. Hydrogen bonds between two water molecules in the solvation layers of ethane are stronger than H–bonds in the bulk of aqueous system [14]. Hydrogen bonds are mutually activated due to the polarization of molecules; i.e., H-bonds between the molecules of water become stronger owing to the electrostatic polarization of the solvation layer.

The absorption of the molecules of organic substances by water clusters still remains scarcely studied. When studying small aqueous systems, it is necessary to take into account the formation of hydrogen bonds between the nearest neighbors. Results of the analysis of the far infrared region of the spectrum of water vapor and clusters performed by the method of density functional testify to the formation of benzene–water dimers [15] and $C_6H_6(H_2O)_9$ clusters [16] in the cooling supersonic jet. The energy of a hydrogen bond in a benzene–

water dimer is estimated as being equal to 1.9 kcal/mol. The interaction between the benzene ring and an $(H_2O)_9$ cluster leads to the formation of one H-bond, as well as considerable change in the distances between oxygen atoms (as well as r_{OH} distances where O and H atoms belong to different molecules) in a cluster. The absorption of C_2H_6 molecules should also lead to the significant structural rearrangement of the entire water cluster. In turn, this should noticeably change the spectral characteristics of aqueous ultradispersed system.

The goal of this work is to study the absorption of ethane molecules by water clusters, to determine the influence of these hydrocarbon molecules on the pattern of the IR spectra of absorption and reflection by aqueous dispersed system, and to establish the role of C_2H_6 molecules in the dissipation of the energy of external IR radiation absorbed by water clusters.

COMPUTER MODEL

The simulation of water clusters was performed using the modified TIP4P interaction potential for water and the rigid four-center model of an H_2O molecule [17]. The geometry of this molecule matches the experimental parameters of a molecule in the gaseous phase; $r_{OH} = 0.09572$ nm and the H–O–H angle is equal to 104.5° [18]. Fixed charges ($q_H = 0.519e$ and $q_M = -1.038e$) are assigned to H atoms in point M at the bisectrix of the HOH angle at a distance of 0.0215 nm from oxygen atom. The values of charges and the position of point M are chosen so as to reproduce experimental values of the dipole and quadrupole moments of water molecules [19, 20], as well as calculated ab initio energy of dimer and characteristic distance in it [21]. The identification of short-range order in water clusters is mainly achieved due to a short-range Lennard-Jones (LD) potential with the interaction center referred to the oxygen atom. The polarizability of a molecule needed for describing the nonadditive part of polarization energy was also referred to point M, along with the electric charge.

The total energy of interaction between water molecules is written in the form

$$U_{\text{tot}}^{(1)} = U_{\text{pair}} + U_{\text{pol}},$$

where the pair-additive part of potential is the sum of Lennard-Jones and Coulombic interactions

$$U_{\text{pair}} = \sum_i \sum_j \left(4\varepsilon \left[\left(\frac{\sigma_{ij}}{r_{ij}} \right)^{12} - \left(\frac{\sigma_{ij}}{r_{ij}} \right)^{6} \right] + \frac{q_i q_j}{r_{ij}} \right).$$

Here, r_{ij} is the distance between points i and j; q is the charge; and σ and ε are the parameters of Lennard-Jones potential.

The nonadditive polarization energy is determined by the relation

$$U_{\text{pol}} = -\frac{1}{2} \sum_i \mathbf{d}_i \mathbf{E}_i^0,$$

where $\mathbf{E}_i^0$ is the strength of electric field in point i induced by the fixed charges of a system

$$\mathbf{E}_i^0 = \sum_{j \neq i} \frac{q_j \mathbf{r}_{ij}}{r_{ij}^3},$$

$\mathbf{d}_i$ is the induced dipole moment of ith atom

$$\mathbf{d}_i = \alpha_i \mathbf{E}_i,$$

where

$$\mathbf{E}_i = \mathbf{E}_i^0 + \sum_{j \neq i} \mathbf{T}_{ij} \mathbf{d}_j.$$

Here, $\mathbf{E}_i$ denotes the total strength of electric field in the center of ith atom, α_i is its polarizability, and $\mathbf{T}_{ij}$ is the dipole tensor

$$\mathbf{T}_{ij} = \frac{1}{r_{ij}^3} \left(\frac{3 \mathbf{r}_{ij} \mathbf{r}_{ij}}{r_{ij}^2} - 1 \right).$$

For the calculation of induced dipole moments at each time step, we used standard iteration procedure [17]. The accuracy of determining $\mathbf{d}_i$ is set in the 10^{-5}–10^{-4} D.

Atom–atom ethane–water interactions were set via the sum of repulsive, dispersion and Coulomb interations

$$\Phi(r_{ij}) = b_i b_j \exp[-(c_i + c_j) r_{ij}] - a_i a_j r_{ij}^{-6} + \frac{q_i q_j}{r_{ij}},$$

where parameters a_i, b_i, and c_i were taken from [22].

Electric charges $q_C^{\text{ethane}} = -0.0939e$ and $q_H^{\text{ethane}} = 0.0313e$ were assigned to C and H atoms, respectively, in ethane molecule. The polarizability of C_2H_6 molecule is referred to the center of its mass (point M). The C_2H_6 molecule has stable conformation in which free rotation around the C–C bond is "retarded" [23]. All H–C–H angles in the ethane molecule are identical and equal to about 109°, whereas the triplet of hydrogen atoms linked with the second carbon atom is turned around the C–C axis by 60° with respect to the triplet of hydrogen atoms retained by the first carbon atom. In this model, the following characteristic distances between atoms in C_2H_6 molecule were used: $r_{CC} = 0.154$ nm and $r_{CH} = 0.11$ nm [24]. In view of the symmetric distribution of electric charge in the C_2H_6 molecule, its permanent dipole moment is equal to zero; however, ethane molecule possesses high polarizability (2.6 Å^3), which is higher than that of water molecule (1.49 Å^3) [24].

Trajectories of the mass centers of molecules were determined by the fourth-order Gear method [25]. Time step Δt of integration was 10^{-17} s. The equilibrium state of water clusters that do not contain admixture molecules at $T = 233$ K was originally established by a molecular dynamic calculation lasted for 2×10^6 Δt. Hereafter, the configuration of water cluster at time moment 20 ps was used as an initial configuration to simulate the $(C_2H_6)_i(H_2O)_n$ system. Added C_2H_6 molecules were originally arranged so that the shortest dis-

tance between atoms in the methane molecule and atoms of water molecules did not exceed 0.6 nm. The C_2H_6 molecule was placed so that the axis of its third-order symmetry would coincide with the ray connecting the center of $(H_2O)_n$ cluster mass with the center of this molecule mass. Cut-off radius r_c of all interactions in the model was 0.9 nm. In the case when two C_2H_6 molecules were added to water cluster, the distance between the centers of these molecules was originally equal to r_c. The relaxation of the newly formed system was performed for 0.6×10^6 Δt time interval; then, required physicochemical properties were calculated for 2.5×10^6 Δt interval. The analytical solution of motion equations for the rotation of molecules was performed using Rodrigues–Hamilton parameters [26] and the scheme of the integration of motion equations in the presence of the rotation of molecules corresponded to the approach proposed by Sonnenschein [27].

Three types of ultradispersed systems were studied. The first system was represented by the water clusters containing 10–20 molecules; the second system consists of $C_2H_6(H_2O)_i$ clusters, $i = 10, \ldots, 20$; the third system composed of the set of $(C_2H_6)_2(H_2O)_i$ clusters containing the same number of H_2O molecules; in the order of their sequence, we designate these systems by numerals I, II, and III. It was assumed that the cluster containing i admixture molecules and n water molecules has the statistical weight

$$W_{in} = \frac{N_{in}}{N_{i\Sigma}}, \quad i = 0, 1, 2, \quad n = 10, \ldots, 20,$$

where N_{in} is the number of clusters with i admixture molecules and n water molecules in 1 cm^3 and $N_{i\Sigma} = \sum_{n=10}^{20} N_{in}$. The N_{in} value was estimated as follows. The case of the scattering of unpolarized light is considered when the mean free path l of molecules is much shorter than the wavelength λ. The extinction (attenuation) coefficient h of the incident beam is determined, on one hand, by the Rayleigh formula [28], and on the other hand, via the scattering coefficient ρ ($h = \frac{16\pi}{3}\rho$) [29] in the approximation of the scattering at an angle of 90°. Taking into account that $h = \alpha + \rho$, where α is the absorption coefficient, we have

$$N_{in} = \frac{2\omega^4}{3\pi c^4}\frac{(\sqrt{\varepsilon}-1)^2}{\alpha}\left(1 - \frac{3}{16\pi}\right),$$

where c is the speed of light, ε is the permittivity of medium, and ω is the frequency of incident wave. All spectral characteristics were calculated with allowance for accepted statistical weights W_{in}. The procedure of the formation cluster systems suggests their uniform spatial distribution and is valid at low cluster concentration; as a consequence, clusters do not interact with each other. The average value of the concentration for the clusters of each type in systems studied is smaller by 12–13 orders of magnitude than the Loschmidt number.

The calculations were performed with a PENTIUM-IV computer operating at a processor clock frequency of 3.8 GHz. The calculation with time 10^6 Δt for the $(C_2H_6)_2(H_2O)_n$ cluster took about 30 h of computer time.

SPECTRAL CHARACTERISTICS OF $(H_2O)_n$ AND $(C_2H_6)_i(H_2O)_n$ CLUSTERS

The total dipole moment of cluster was calculated by the formula

$$\mathbf{M}(t) = \sum_{i=1}^{N} \mathbf{d}_i(t),$$

where $\mathbf{d}_i(t)$ is the dipole moment of molecule i and N is the number of molecules in a cluster.

Static dielectric constant ε_0 was determined via the fluctuations of the total dipole moment [30]

$$\varepsilon_0 = 1 + \frac{4\pi}{3VkT}[\langle \mathbf{M}^2 \rangle - \langle \mathbf{M} \rangle^2],$$

where V is the volume of a cluster.

Let us introduce the transformation of Fourier–Laplace function f via the relation

$$L_{i\omega}[f] = \int_0^\infty dt e^{-i\omega t} f(t)$$

and normalized autocorrelation function $\mathbf{M}$ using the equality

$$\Phi(t) = \langle \mathbf{M}(0)\mathbf{M}(t) \rangle / \langle \mathbf{M}^2 \rangle.$$

Frequency dependence of permittivity is represented as the complex value $\varepsilon(\omega) = \varepsilon'(\omega) + i\varepsilon''(\omega)$ with the real part $\varepsilon'(\omega)$ (dielectric dispersion) and the imaginary part $\varepsilon''(\omega)$ characterizing dielectric losses. Then the relation between the frequency-dependent dielectric constant and the Fourier–Laplace transformation for the derivative with respect to time of function Φ is determined by the relation [31]

$$L_{i\omega}[-\dot{\Phi}] = \frac{\varepsilon(\omega) - 1}{\varepsilon_0 - 1} = 1 - i\omega L_{i\omega}[\Phi].$$

The ε_0 value is calculated through function $\varepsilon(\omega)$: $\varepsilon_0 = \varepsilon(0)$.

The molecule can absorb electromagnetic waves with a specific frequency only in the case when the dipole moment of a molecule vibrates with the same frequency. The absorption coefficient is proportional to the squared amplitude of the vibration of the dipole moment. The absorption of radiation at frequency ω at thermodynamic equilibrium in the gaseous phase with

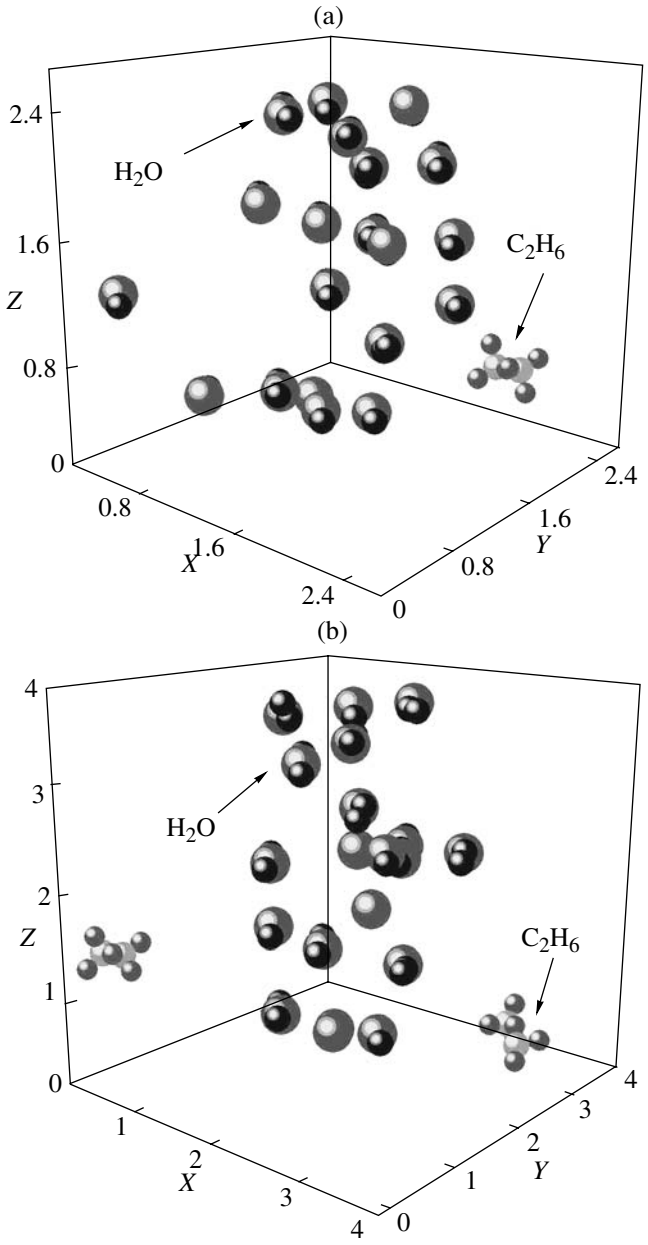

Fig. 1. Configurations of the clusters corresponding to a time of 25 ps: (a) $C_2H_6(H_2O)_{20}$ and (b) $(C_2H_6)_2(H_2O)_{20}$ clusters.

temperature T is characterized by absorption coefficient α. The α can be presented via the imaginary part of frequency-dependent permittivity $\varepsilon(\omega)$ in the following form [31]:

$$\alpha(\omega) = 2\frac{\omega}{c}\mathrm{Im}[\varepsilon(\omega)^{1/2}],$$

where c is the speed of light.

Reflection coefficient R was determined as the ratio of the average energy flux reflected by the surface to the incident flux. For a normal incidence of a plane monochromatic wave, the reflection coefficient is given by the equation [28]

$$R = \left|\frac{\sqrt{\varepsilon_1} - \sqrt{\varepsilon_2}}{\sqrt{\varepsilon_1} + \sqrt{\varepsilon_2}}\right|^2. \quad (1)$$

Here, it is assumed that the incidence of the wave occurs from a transparent medium (medium 1) to a medium, which can be transparent or opaque, i.e., absorbing or scattering (medium 2). Subscripts at the permittivity in Eq. (1) refer to the corresponding media.

Frequency dependence of dielectric losses $P(\omega)$ can be expressed as [29]

$$P = \frac{\varepsilon''\langle E^2\rangle\omega}{4\pi},$$

where $\langle E^2\rangle$ is the average value of the squared strength of electric field and ω is the frequency of emitted electromagnetic wave.

The total number of electrons N_e per unit volume of a cluster interacting with the external electromagnetic field is set as [28]

$$N_e = \frac{m}{2\pi^2 e^2}\int_0^\infty \omega\varepsilon''(\omega)d\omega,$$

where e and m are the charge and the mass of electron, respectively.

CALCULATION RESULTS

The configurations of $C_2H_6(H_2O)_{20}$ and $(C_2H_6)_2(H_2O)_{20}$ clusters obtained at time 25 ps are presented in Fig. 1. The C_2H_6 molecules are not detached by the water core of a cluster; however, at the same time, they do not approach the core too closely. In the case of both clusters, every C_2H_6 molecule is adjacent to three water molecules. In addition, every C_2H_6 molecule is oriented arbitrarily to the water core of a cluster; i.e., its C–C axis is directed neither at the center of a cluster mass nor tangentially to the core "surface." The presence of a second C_2H_6 molecule changes the shape of the water skeleton of a cluster. This is associated with the fact that every ethane molecule adjusts the nearest water molecules of cluster to its conformation. The C_2H_6 molecules are quite remote from water molecules as compared to the distance between the adjacent H_2O molecules. In general, the surface of the $(C_2H_6)_2(H_2O)_{20}$ cluster turned out to be looser than the surface of $C_2H_6(H_2O)_{20}$ cluster.

Static permittivity ε_0 demonstrates how many times the field of free charge in a dielectric is reduced with respect to vacuum. The $\varepsilon_0(n)$ functions calculated in the $10 \le n \le 20$ range for the clusters of pure water and for the clusters added one or two C_2H_6 molecules are shown in Fig. 2. The hydrophobic interaction between H_2O and C_2H_6 molecules leads to some compaction of

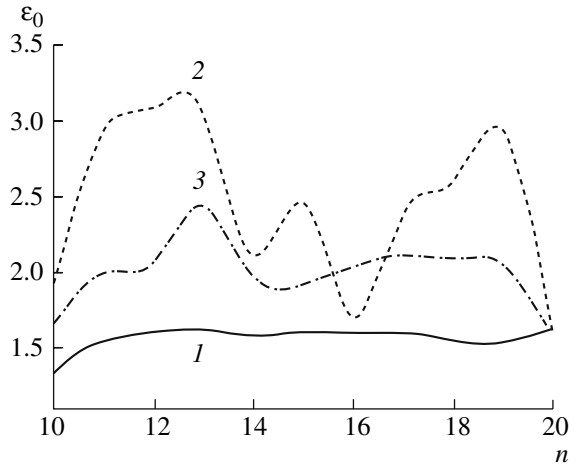

Fig. 2. Dependences of the static permittivity of clusters on the number of water molecules in clusters: (*1*) $(H_2O)_n$, (*2*) $C_2H_6(H_2O)_n$, and (*3*) $(C_2H_6)_2(H_2O)_n$.

water volume of heteroclusters, which resulted in an increase in the ε_0 values. At the same time, large fluctuations of ε_0 values are observed with changes in the sizes of heteroclusters, in particular, in the case when only one C_2H_6 molecule is present in aggregates. The addition of the second C_2H_6 molecule leads to a more uniform distribution of water molecules and a decrease in the level of the fluctuations of $\varepsilon_0(n)$ function.

Frequency dependences of the real and imaginary parts of dielectric permittivity for a system of clusters of pure water (system I), as well as for an aqueous ultradispersed system, each cluster of which contains one (system II) or two (system III) C_2H_6 molecules, are shown in Fig. 3. The addition of C_2H_6 molecules to water clusters results in a decrease in the ε' and ε'' values for ultradispersed systems. Moreover, the higher the ethane concentration in a system of water clusters, the lower the ε' and ε'' values for a system. This regularity is traced throughout the frequency range for the real part of dielectric permittivity and almost over the entire (except for frequencies $\omega < 25$ cm^{-1}) frequency range for the imaginary part of ε. The ε' value for bulk liquid water [32] rapidly decreases with frequency and, at $\omega >$ 180 cm^{-1}, becomes smaller than the corresponding characteristic for the ultradispersed systems under consideration. For bulk water, the experimental frequency dependence of ε'' [33] decays slower with an increase in frequency and, at $\omega > 860$ cm^{-1}, the ε'' value becomes lower than for the studied ultradispersed systems.

After the absorption of ethane, the absorption of external IR radiation by aqueous ultradispersed systems within the $0 \le \omega \le 1000$ cm^{-1} frequency range rises (Fig. 4) and the pattern of $\alpha(\omega)$ curve becomes smoother. However, the doubled C_2H_6 concentration leads to some decrease in the absorption of IR radiation, at least at frequencies $\omega > 310$ cm^{-1}. Nevertheless, almost throughout the frequency range (except for the

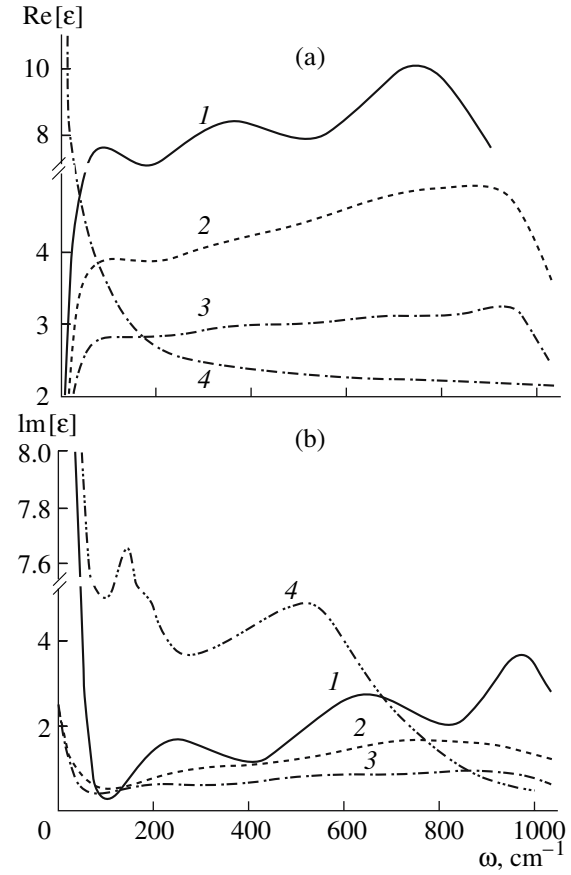

Fig. 3. Frequency dependences of (a) real and (b) imaginary parts of dielectric permittivity of ultradispersed systems: (*1*) system I, (*2*) system II, (*3*) system III, and (*4*) molecular dynamic calculation for (a) bulk water [32] and (b) experimental results for liquid water [33].

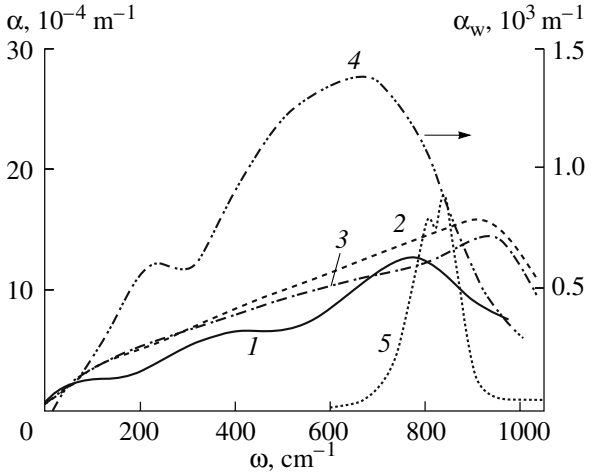

Fig. 4. Frequency dependences of the IR absorption coefficient for various systems: (*1*) system I, (*2*) system II, (*3*) system III, (*4*) bulk water, experiment [34], and (*5*) experimental spectrum for the gaseous C_2H_6 [35]. The arrow indicates the ordinate axis for spectrum 4.

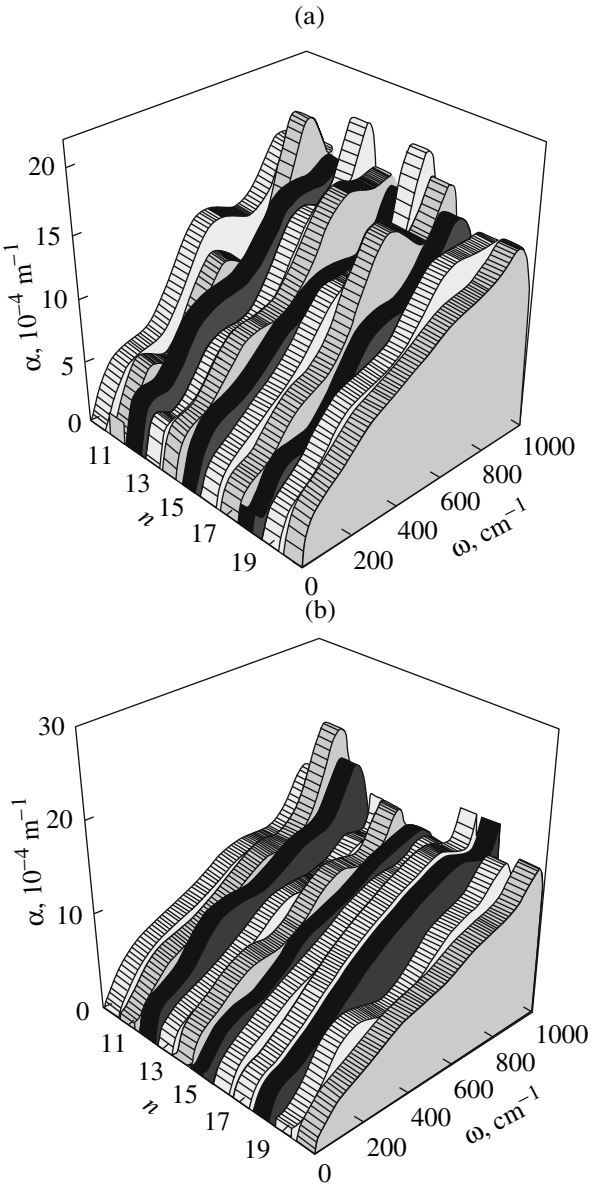

Fig. 5. The IR absorption spectra of various clusters: (a) $C_2H_6(H_2O)_n$ and (b) $(C_2H_6)_2(H_2O)_n$.

$690 \le \omega \le 800$ cm^{-1} range), the values of coefficient α are larger for system III than for system I. The major maximum of frequency spectrum $\alpha(\omega)$ shifts from position $\omega = 784$ cm^{-1} for system I to position $\omega = 910$ cm^{-1} for system II and to $\omega = 973$ cm^{-1} for system III. The $\alpha_w(\omega)$ spectrum for bulk water [34] is characterized by two maxima at frequencies $\omega = 200$ and 700 cm^{-1}; for the gaseous ethane, by the splitted maximum in the $810 \le \omega \le 840$ cm^{-1} frequency range.

Variations in the absorption coefficient with frequency for every cluster of systems II and III are shown in Fig. 5. In general, clusters of system II, i.e., clusters containing one C_2H_6 molecule each, are characterized by larger oscillations of coefficient α than clusters containing two C_2H_6 molecules each, i.e., clusters that belong to system III. Note also that when passing from one cluster to another, the integral absorption intensity of IR radiation changes to a smaller extent for system III.

The addition of C_2H_6 molecules to water clusters leads to a substantial change in the reflection IR spectra for ultradispersed systems (Fig. 6). The intensity of the $R(\omega)$ spectra lowers and to a larger extent, the larger amount of ethane molecules is absorbed by the ultradispersed system. Average intensities of the reflection of IR radiation for systems I, II, and III are equal to 0.23, 0.12, and 0.07, respectively. The spectra of systems II and III containing C_2H_6 molecules becomes band spectra. Moreover, the number of peaks in the $R(\omega)$ spectrum is almost doubled, from 10 for system I to 19 for systems II and III. Furthermore, peaks in the $R(\omega)$ spectrum of ultradispersed systems become more resolved.

The character of changes in the coefficient of reflection of the IR radiation with frequency for every cluster of systems II and III is illustrated by Fig. 7. The reflection for single clusters of system II is characterized by considerable nonuniformity. For example, the average reflection coefficient for $C_2H_6(H_2O)_n$ clusters with n = 11, 12, 13, 15, and 19 varies from 0.12 to 0.15, while at n = 14, 16, and 20, it does not exceed 0.03. The intensities of $R(\omega)$ spectra for different clusters are balanced with the addition of a second C_2H_6 molecule to clusters; however, on average, the reflection of IR radiation becomes less intense.

Clusters of water, including those that absorb C_2H_6 molecules, can reemit the absorbed IR radiation. Power P of cluster emission substantially lowers after they absorbed ethane molecules (Fig. 8a). In this case, $P(\omega)$ spectra for systems II and III become smoother than for system I. The doubling of the number of C_2H_6 molecules in the ultradispersed system leads to some increase in the power of radiation. Integral intensities of the radiation power for systems I, II, and III are in the ratio of 1 : 0.33 : 0.6. Major minima of $P(\omega)$ spectra for systems I, II, and III are localized at ω = 973, 847, and 910 cm^{-1}, respectively. The behavior of maximum value P_{max} as being dependent on the number of molecules in the clusters is shown in Fig. 8b. Almost everywhere, the P_{max} values for clusters of system III are larger than those for clusters of system II. The reverse relation is observed only at n = 20. At the same time, P_{max} value for clusters of pure water is lower than that for clusters containing ethane molecules except for water clusters with n = 10, 16, and 20, for which the values of statistical weights are in the ratio of 1 : 2.7 : 106.6. It is worth mentioning that the P_{max} value for water clusters with n = 10 and 16 is only slightly larger than the corresponding characteristic for clusters that capture one ethane molecule, whereas at n = 20, an increase in P_{max} value becomes significant upon the capture of one or two ethane molecules. As the ethane

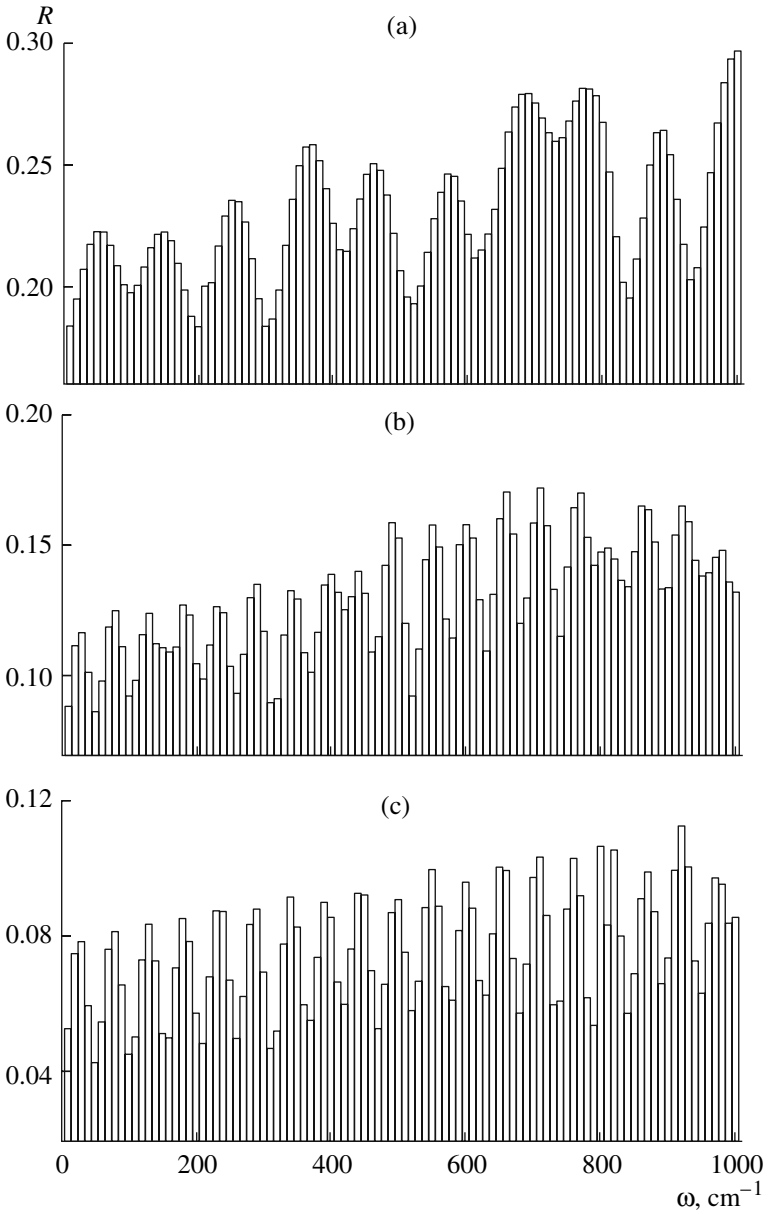

Fig. 6. Frequency dependences of the IR reflectance spectra for systems (a) I, (b) II, and (c) III.

concentration increases, variations in P_{max} values become less significant.

The density of electrons N_{el} interacting with the electromagnetic wave passing through the clusters, in the case of system I, is characterized by the largest oscillations when passing from one cluster to another (Fig. 9). When C_2H_6 molecules are added to clusters, oscillations of the N_{el} value related to the variations in the number of molecules in the aggregate are smoothed. Moreover, as the number of ethane molecules in the ultradispersed system doubles, the average N_{el} value is not increased; $\overline{N}_{el} = 0.8 \times 10^{14}$ cm^{-3} and 0.6×10^{14} cm^{-3} for systems II and III, respectively. Among all studied clusters, the cluster of pure water containing 20 molecules has the largest N_{el} value that is related to the most open (dodecahedral) structure of this aggregate.

CONCLUSIONS

Clusters containing 10–20 water molecules can absorb one or two ethane molecules without a loss of stability. This is evidenced by the positive value of derivative $(\partial\mu/\partial n)_{V,T}$, where μ is the chemical potential. In the $140 \le \omega \le 1000$ cm^{-1} frequency range, the values

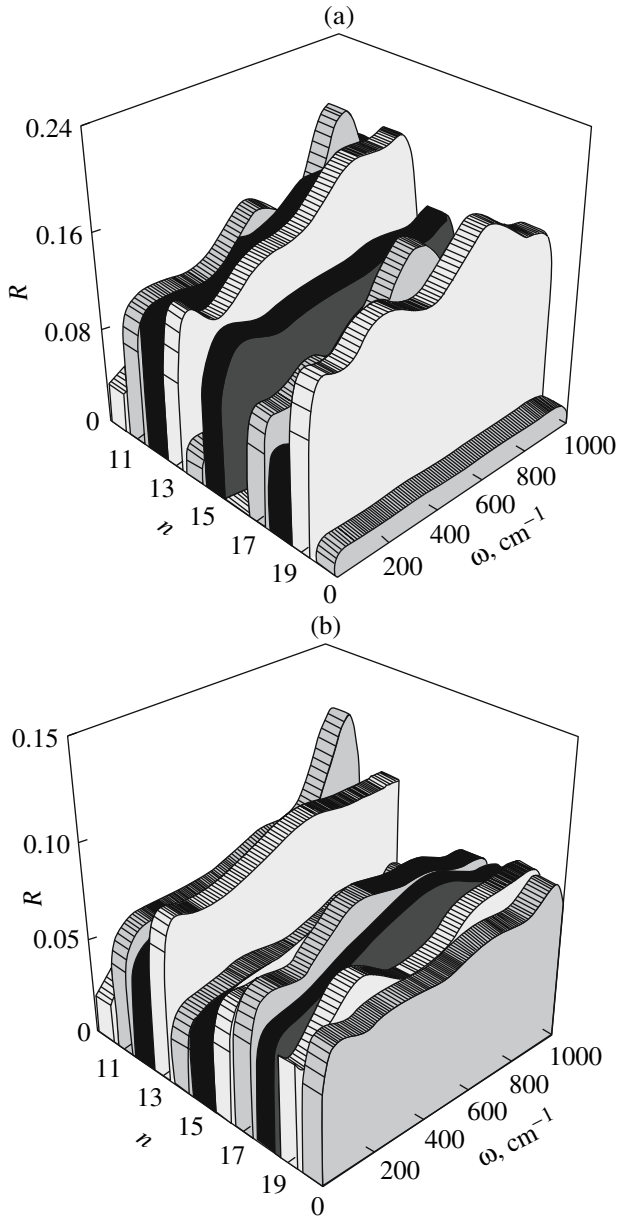

Fig. 7. The IR reflectance spectra of various clusters: (a) $C_2H_6(H_2O)_n$ and (b) $(C_2H_6)_2(H_2O)_n$.

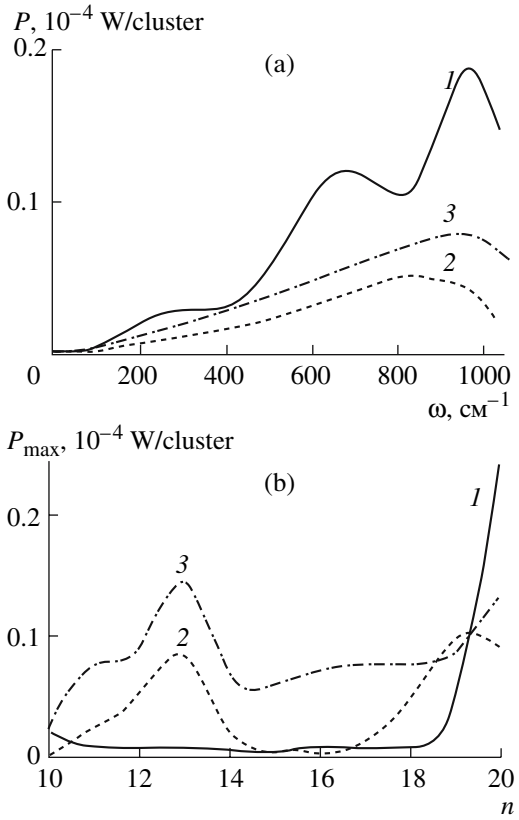

Fig. 8. (a) Frequency dependences of the power of IR radiation $P(\omega)$ for (*1*) I, (*2*) II, and (*3*) III systems and (b) the dependences of maximum P value on the number of water molecules n in clusters for the same systems (designations are the same as before).

of both real and imaginary parts of dielectric permittivity decrease after the absorption of C_2H_6 molecules by the aqueous ultradispersed system. In the same frequency range, the integral coefficient of IR absorption by ultradispersed medium rises due to the absorption of C_2H_6 molecules by the clusters of water molecules. However, the doubling of the ethane concentration in the ultradispersed system leads to a decrease in the absorption of thermal radiation. After the absorption of C_2H_6 molecules by aqueous ultradispersed system, its spectrum of the reflection of IR radiation substantially changes. From continuous for ultradispersed system, this spectrum becomes the band spectrum for a system containing ethane. Water clusters that absorb C_2H_6 molecules lower their ability for the IR radiation. The ultradispersed system composed of such clusters decreases the power of heat emission. However, as the ethane concentration increases, the power of IR radiation rises and the maximum of emitted power shifts again toward the localization of corresponding maximum for the ultradispersed system of pure water. The cluster of pure water composed of 20 molecules is characterized by the highest power of IR radiation. Among the clusters of system II, the same property is exhibited by $C_2H_6(H_2O)_{19}$ cluster; system III, by $(C_2H_6)_2(H_2O)_{13}$ cluster. The density of electrons interacting with the electromagnetic wave changes significantly after the absorption of C_2H_6 molecules by clusters. For clusters containing ethane molecules, a dip is formed on the $N_{el}(n)$ dependence in the $14 \le n \le 16$ size range where the maximum of N_{el} was observed for the ultradispersed system of pure water.

The absorption of ethane molecules by water clusters leads to some increase in the absorption of IR radiation; however, no complete compensation occurs for the corre-

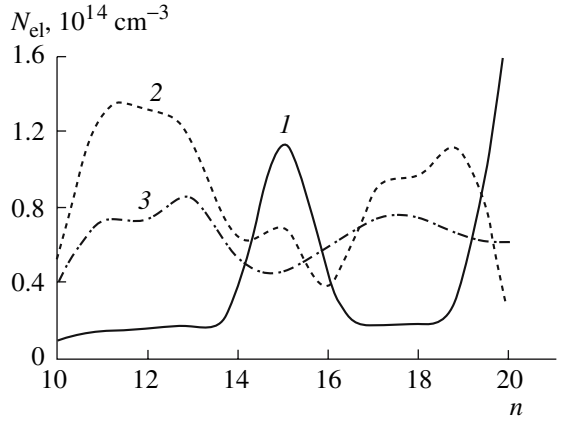

Fig. 9. Dependences of the density of electrons interacting with electromagnetic wave in clusters on the number of cluster-constituting molecules (*1*) $(H_2O)_n$, (*2*) $C_2H_6(H_2O)_n$, and (*3*) $(C_2H_6)_2(H_2O)_n$.

sponding absorption by free C_2H_6 molecules. Because of this, the greenhouse effect caused by the absorption of low-frequency IR radiation ($0 \le \omega \le 1000$ cm^{-1}) decreases.

ACKNOWLEDGMENTS

This work was supported by the Presidium of Ural Branch of the Russian Academy of Sciences, the grant for the research project for young scientists and graduate students.

REFERENCES

1. El'yashevich, M.A., *Atomnaya i molekulyarnaya spektroskopiya* (Atomic and Molecular Spectroscopy), Moscow: Fizmatlit, 1962.
2. Stern, H.A. and Berne, B.J., *J. Chem. Phys.*, 2001, vol. 115, p. 7622.
3. Pfeilsticker, K., Lotter, A., Peters, C., and Bosch, H., *Science* (Washington, D.C.), 2003, vol. 300, p. 2078.
4. Ptashnik, I.V., Smith, K.M., Shine, K.P., and Newnham, D.A., *Q. J. R. Meteorol. Soc.*, 2004, vol. 130, p. 2391.
5. Burch, D.E., AFGL-TR-85-0036.
6. Ptashnik, I.V., *Opt. Atmos. Okeana*, 2005, vol. 18, p. 359.
7. Volmer, M., *Kinetika obrazovaiya novoi fazy* (The Kinetics of New Phase Formation), Moscow: Nauka, 1986.
8. Mhin, B.J., Lee, S.J., and Kim, K.S., *Phys. Rev. A,* 1993, vol. 48, p. 3764.
9. Jorgensen, W.L., Chandrasekhar, J., Madura, J.D., et al., *J. Chem. Phys.*, 1983, vol. 79, p. 926.
10. Mahoney, M.W. and Jorgensen, W.L., *J. Chem. Phys.*, 2000, vol. 112, p. 8910.
11. Praprotnik, M. and Janezic, D., *J. Chem. Phys.,* 2005, vol. 122, p. 174103.
12. Guillot, B., *J. Mol. Liq.*, 2002, vol. 101, p. 219.
13. Praprotnik, M., Janezic, D., and Mavri, J., *J. Phys. Chem., A*, 2004, vol. 108, p. 11 056.
14. Xu, H., Stern, H.A., and Berne, B.J., *J. Phys. Chem., B*, 2002, vol. 106, p. 2054.
15. Suzuki, S., Green, P.G., Bumgarner, R.E., et al., *Science* (Washington, D. C.), 1992, vol. 257, p. 942.
16. Gruenloh, C.J., Carney, J.R., Hagemeister, F.C., and Zwier, T.S., *J. Chem. Phys.*, 2000, vol. 113, p. 2290.
17. Dang, L.X. and Chang, T.-M., *J. Chem. Phys.*, 1997, vol. 106, p. 8149.
18. Benedict, W.S., Gailar, N., and Plyler, E.K., *J. Chem. Phys.*, 1956, vol. 24, p. 1139.
19. Xantheas, S., *J. Chem. Phys.*, 1996, vol. 104, p. 8821.
20. Feller, D. and Dixon, D.A., *J. Phys. Chem.*, 1996, vol. 100, p. 2993.
21. Smith, D.E. and Dang, L.X., *J. Chem. Phys.*, 1994, vol. 100, p. 3757.
22. Spackman, M.A., *J. Chem. Phys.*, 1986, vol. 85, p. 6579.
23. Morse, J.K., *Physics*, 1928, vol. 14, p. 37.
24. *Spravochnik khimika* (Chemist's Handbook), Nikol'skii, B.P., Ed., Leningrad: Khimiya, 1971.
25. Haile, J.M., *Molecular Dynamics Simulation. Elementary Methods*, New York: Wiley, 1992.
26. Koshlyakov, V.N., *Zadachi dinamiki tverdogo tela i prikladnoi teorii giroskopov* (Problems of Dynamics of Solids and Applied Theory of Gyroscopes), Moscow: Nauka, 1985.
27. Sonnenschein, R., *J. Comput. Phys.*, 1985, vol. 59, p. 347.
28. Landau, L., Lifshitz, E., and Pitaevski, L., *Electrodynamics of Continuous Media*, Oxford: Pergamon, 1984.
29. *Fizicheskaya entsiklopediya, tom 1*, (Physical Encyclopedia, vol. 1), Prokhorov, A.M., Ed., Moscow: Sovetskaya Entsiklopediya, 1988.
30. Bresme, F., *J. Chem. Phys.*, 2001, vol. 115, p. 7564.
31. Neumann, M., *J. Chem. Phys.*, 1985, vol. 82, p. 5663.
32. Neumann, M., *J. Chem. Phys.*, 1986, vol. 85, p. 1567.
33. Angell, C.A. and Rodgers, V., *J. Chem. Phys.*, 1984, vol. 80, p. 6245.
34. Goggin, P.L. and Carr, C., in *Water and Aqueous Solutions*, Neilson, G.W. and Enderby, J.E., Eds., Bristol: Adam Hilger, 1986, vol. 37, p. 149.
35. Kozintsev, V.I., Belov, M.L., Gorodnichev, V.A., and Fedotov, Yu.V., *Lazernyi optiko-akkusticheskii analiz mnogokomponentnykh gazovykh smesei* (Laser Optical-Acoustic Analysis of Multicomponent Gas Mixtures), Moscow: Mosk. Gos. Tekh. Univ., 2003.